Available online at www.sciencedirect.com
ScienceDirect
Engineering Failure Analysis 14 (2007) 1594–1604
ENGINEERING FAILURE ANALYSIS
www.elsevier.com/locate/engfailanal

Investigation of low temperature effects on fatigue behavior of PVDF

A. Al-Abduljabbar [a,*], B. Melve [b], N. Dodds [c], A.G. Gibson [c]

[a] Department of Mechanical Technology, Riyadh College of Technology, GOTEVOT, P.O. 20129, Riyadh 11455, Saudi Arabia
[b] Statoil Research Centre, Statoil ASA, Arkitekt Ebbelsvei 10, Rotvoll, N-7005 Trondheim, Norway
[c] Department of Mechanical Engineering, University of Newcastle Upon Tyne, Newcastle, UK

Received 15 October 2006; accepted 30 November 2006
Available online 27 December 2006

Abstract

Fatigue behavior of polyvinylidiene fluoride (PVDF) pipes is investigated under low temperatures to characterize the temperature effects. The analysis included experimental evaluation of fatigue life for test samples taken directly from the manufactured pipes used for service as opposed to compression molded compact tension samples used in previous works. In this test, short sections from an extruded pipe are used to better represent the material service conditions. A compact test chamber was designed to control the test temperature. The samples were loaded into the test rig and allowed to cool for 30 min ensuring a constant and even temperature distribution. Cooling was done in a sealed test chamber using carbon dioxide gas. Two test temperatures of −20 °C and −10 °C were chosen since they represent typical temperature during which failure occurs during actual pipe service in cold environments. Fractured surfaces were inspected and fatigue data were analyzed using a standard procedure for calculation of fatigue life with a semi-elliptical surface crack assumption was performed; from which parameters of the Paris law for fatigue fracture were obtained. Comparing the results with previous works it is found that they capture the trend of the PVDF material behavior for high temperature.
© 2007 Elsevier Ltd. All rights reserved.

Keywords: Fatigue; Fracture; Polyvinylidiene fluoride (PVDF); Stress intensity factor; Temperature effect

1. Introduction

Polyvinylidiene fluoride (PVDF) is a semi-crystalline thermoplastic that has superior chemical resistance properties and can be extruded easily. These favorable features give it wide applications in the oil, gas and chemical industries as an impermeable liner material in high temperature operation of underwater flexible pipes. During service, when the PVDF-containing flexible pipe is subjected to sequences of loading and unloading, it undergoes noticeable change in temperature. As a result, thermally induced fatigue cracks are thought to propagate through the PVDF liner material. Fatigue crack propagation causes failure which has been attributed to temperature fluctuations that occur during the service life of the pipe riser.

* Corresponding author. Tel.: +966 50 5164049; fax: +966 1 4939924.
E-mail address: aajabbar@gmail.com (A. Al-Abduljabbar).

1350-6307/$ - see front matter © 2007 Elsevier Ltd. All rights reserved.
doi:10.1016/j.engfailanal.2006.11.076

The approach to investigate this fatigue failure problem starts with reviewing works on effects of temperature variations on the fatigue and in general, and in particular PVDF and semi-crystalline thermoplastics. Hertzberg and his coworkers [1,2] addressed this problem by considering effects of test frequency on fatigue behavior of various polymers and suggested that there are competing effects of strain rate hardening and creep damaging on the fatigue response of polymers, with different polymers showing different sensitivity levels to frequency at different temperatures. The superior fatigue behavior of crystalline polymers over amorphous polymers was attributed to the stronger structure of the former, and the effect of the frequency is explained through the rising temperature at the advancing crack tip. From testing different polymers, including PVDF, nylon 6,6 and ployacetal distinction between the characteristics of fatigue fracture mechanisms at temperatures below and above the transition temperature T_g.

Grieg [3] preformed fatigue testing of compact tension specimens of compression molded PVDF samples; at ambient and elevated temperatures. He pointed out to the effect of test frequency on heating the crack tip zone, thus complicating the temperature effects on the fatigue behavior of the material; and suggested a specific maximum value for the test frequency. In another work, Melve [3] presented a methodology to predict failure due to crack growth in PVDF pressure barriers in flexible risers based on the fatigue fracture equation of Paris law. Gibson and Jerry [5] proposed a model to work out Melve's methodology and produce results that can be compared with actual fracture data. The model has taken into account additional effects such as stable crack growth and creep. Merah and coworkers [6] studied the combined effects of test frequency and temperature on the fatigue behavior of chlorinated polyvinyl chloride (CPVC), using single notched specimens. They concluded that the effect of temperature is to increase the crack growth rate independent of the frequency, and that frequency had the opposite effect.

During service of flexible pipe containing PVDF, very low temperatures are encountered at which there is no fatigue data. The aim of this work is to investigate the effect of low temperature on the fatigue behavior of PVDF and correlate such temperature effect to the established relations such as the Paris law. This work will utilize experimental testing described herein to devise analytic interpretation of the fatigue fracture behavior of PVDF at low temperatures.

2. Experimental

The experimental set up for this project required a specific design for the test apparatus, since the testing of PVDF samples is going to be conducted at very low temperatures. Also, test samples are different from those used in above mentioned works in the fact that they are taken directly from the manufactured extruded pipes which are used for actual service. In what follows, brief descriptions about these two issues, as well as the test procedure that was conducted, are presented.

Previous fatigue testing of PVDF used compression molded compact tension samples of the material. In this test, short sections from an extruded pipe are used to better represent the material service conditions. Worthy of mention is presence of residual stresses in the extruded pipe from which the samples are taken, as a result of the extrusion process. For this reason, the internal surfaces of the samples were machined to relieve most of the residual stresses. Samples were cut and finished with a radial thickness of 6 mm, a width of 20 mm, and an internal radius of 95 mm. Fig. 1 shows a finished sample held with one holder of the test apparatus.

To ensure a tight grip on the sample test and a fully tensile loading of the sample, semicircular D shaped holders are used to constitute the grip on the sample as shown in diagram of Fig. 2. This shape was chosen so that the test samples would be allowed to retain its circular shape. Moreover, a compact test chamber is needed to control the test temperature. A compact rig design was also required to fit within the confined space of the test chamber. The main holders consisted of cylindrical bar stock with a slot cut through each of them between which the test samples would be constrained. Fig. 3 shows a photograph of a fully assembled rig with sample loaded for testing.

Samples were loaded into the test rig and allowed to cool for 30 min ensuring a constant and even temperature distribution. Cooling was done in a sealed test chamber using carbon dioxide gas. Two test temperatures of −20 °C and −10 °C were chosen since they represent typical temperature during which blowdown occurs during actual pipe service. Table 1 shows the samples used in this analysis. A constant amplitude cyclic load

Fig. 1. Photograph of the sample held by one holder.

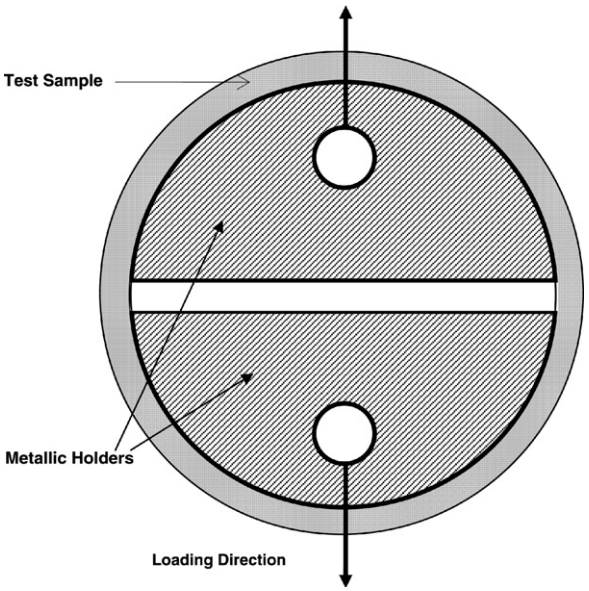

Fig. 2. Diagram of the holder design of the sample.

setting was input for computer control. Samples were subjected to tension–tension loading of between 75% and 95% of their yield strength at each temperature. A low constant frequency of 0.5 Hz was selected to minimize the effects of localized heating of the stress region, [3]. An Instron 20 kN load cell was used. In addition, a computer connected to the Instron 8500 was used to control the frequency, displacement, waveform, maximum and minimum loads. As well as to record the crosshead data points and the number of cycles completed.

To help make scanning electronic microscope analysis of the fractured surfaces, samples were cut half inch from one of the fractured surfaces. Photographs in Fig. 4a and b show samples tested at temperatures −20 °C, and −10 °C, respectively. The photographs are included to demonstrate crack surface shape and relate this to SEM graphs. SEM graphs for samples tested at −20 °C, are shown in Fig. 5. From comparison of Fig. 5a which shows an SEM photograph for the crack face of the sample magnified up to 50 times (50×), with the top sample in Fig. 4a, the general surface characteristics can be observed. Fig. 5b shows an SEM photograph for the crack face of the same sample in Fig. 5a but with a magnification of 500×, which reveals the striations

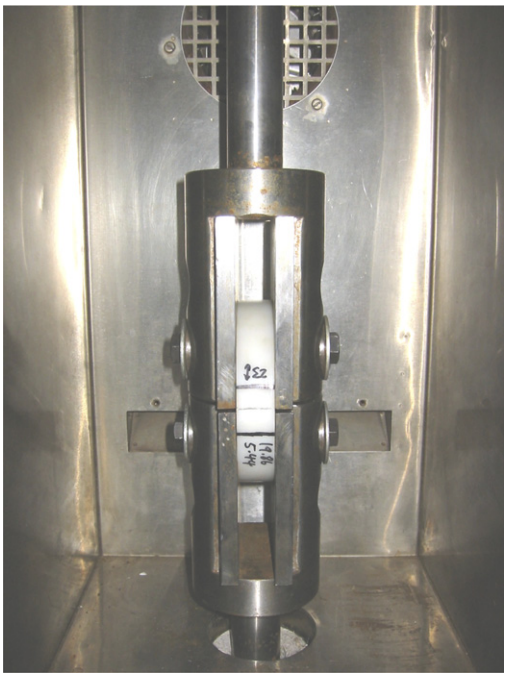

Fig. 3. Assembly of the test rig.

Table 1
Test samples used in the analysis, and corresponding test temperatures

Sample	Temperature (°C)
PVDF7	−20
PVDF8	−20
PVDF20	−10
PVDF22	−10

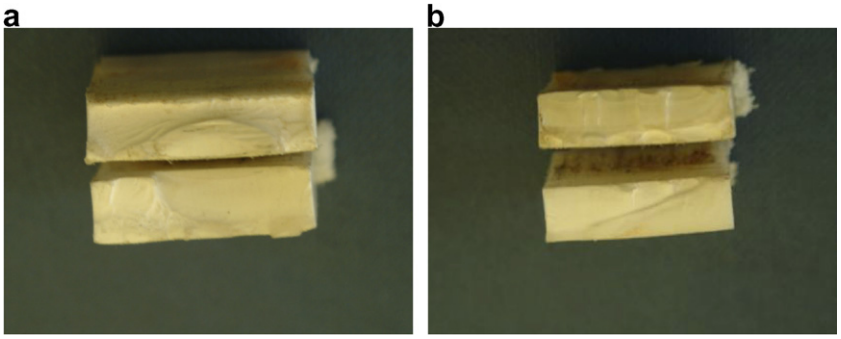

Fig. 4. Photographs of samples tested at −20 °C and −10 °C. The photograph shows the crack face of (a) samples 7 (top) and 8, and (b) samples 20 (bottom) and 22 (top) after being cut from the sample. The crack propagation direction is from the inner side (top of each sample) to the outer side (bottom).

representing cyclic loading on the specimen with crack fatigue growth. SEM photographs of bottom sample in Fig. 4b are shown in Fig. 5c for a magnification of 50×, and Fig. 5d for a magnification of 500×. The SEM photographs are compared with camera photographs to confirm the proper direction of crack propagation.

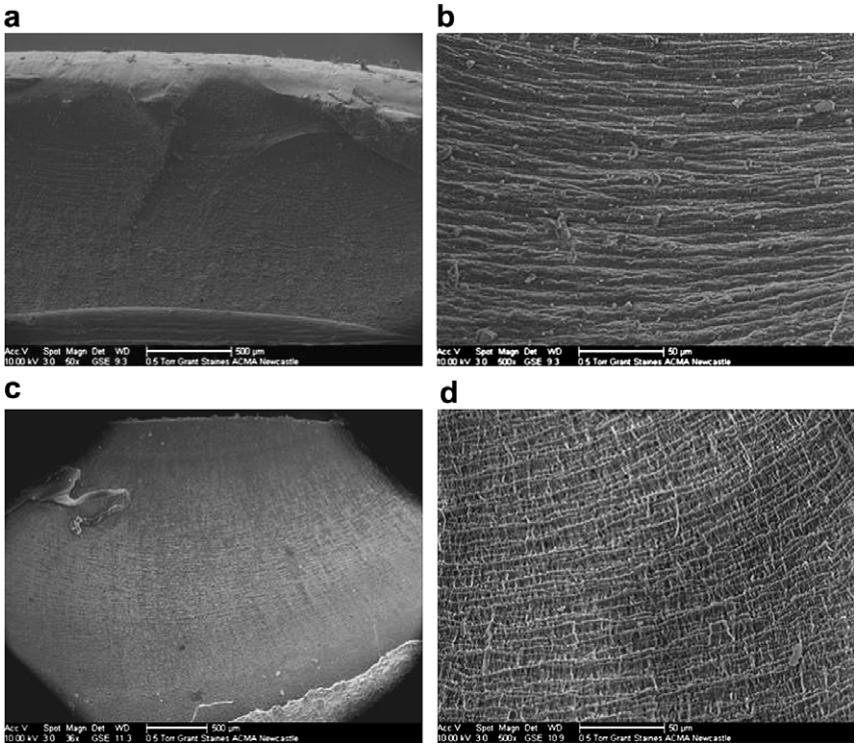

Fig. 5. Scanning microscope of samples tested at −20 °C, of sample 7 magnified up to 50× (a), and 500× (b), and Sample 8 with 32× magnification (c) and 500× magnification (d); with inner surface (start of crack initiation and propagation) at the top. This can be confirmed by comparison with the sample in Fig. 4a.

Crack parameters are estimated from these photographs so that they are used later on to predict the fatigue fracture model for the material based on the experimental tests conducted.

Similarly, SEM photographs of samples tested at −10 °C are shown in Fig. 6 (SEM photographs Fig. 6a and b for the sample at the top of Fig. 4b, and photographs Fig. 6c and d for sample at the bottom of Fig. 4b). For each case, comparison with the camera photographs confirms the crack surface shape in the same way discussed above. The SEM photographs of Figs. 5 and 6 are analyzed to estimate the fatigue crack parameters required to construct the fatigue crack relations of Paris law.

3. Analysis

3.1. Stress intensity factor

From inspection of SEM photographs of fractured samples, the crack is assumed to be semi-elliptical surface crack in an infinite plate. As indicated by Melve [4] the semi-elliptical crack shape assumption is more realistic when representing the crack initiation, than that of a straight crack. Assuming a semi-elliptical surface crack within an infinite plate requires the estimate the crack half length (c), in addition to crack depth (a). The stress intensity factor is obtained from the following relation

$$K_{\mathrm{I}} = \sigma_{\infty}\sqrt{\pi\frac{a}{Q}}Y(a,c,\phi). \tag{1}$$

For this case, the geometry factors Y and Q are calculated based on the work of Newman and Raju [7] and Anderson [8]. A series of parameters are calculated using a, c, specimen thickness t, width b, and the parametric angle of the ellipse ϕ. Since Y is a function of ϕ for a the whole range of the semi-ellipse, with the maximum

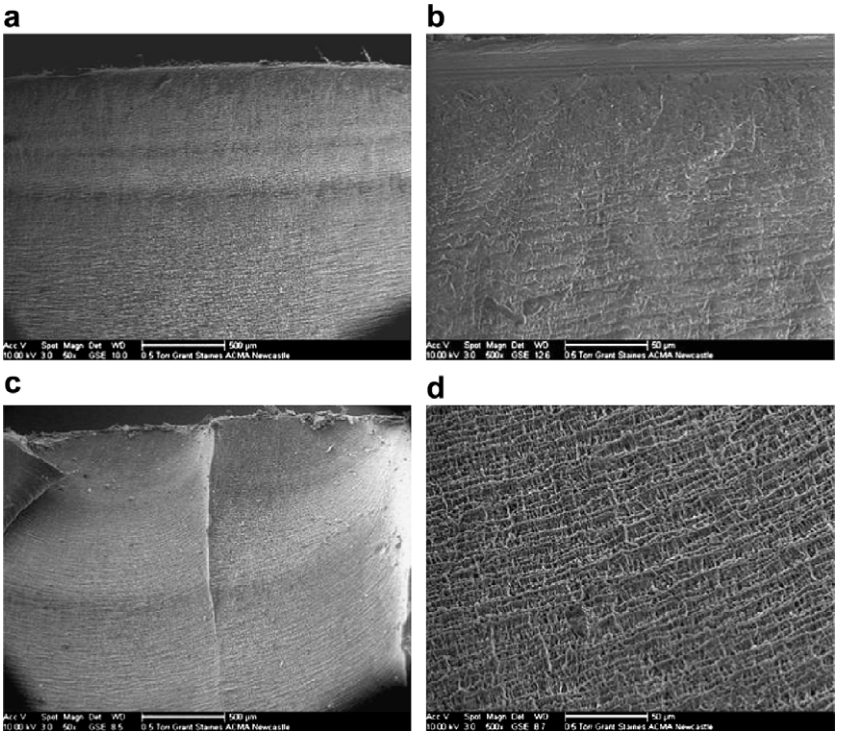

Fig. 6. Scanning microscope graphs of samples tested at −10 °C, sample 20 with 50× (a) and 500× magnification (b). and sample 22 with 50× (c) and 500× magnification (d).

value corresponding to an angle of 90°, this value is used in the calculation of Y as it is the most sensitive case. The geometry factor Y is given by the following relation

$$Y(a,c,\phi) = \left[M_1 + M_2\left(\frac{a}{t}\right)^2 + M_3\left(\frac{a}{t}\right)^4\right] f_\phi g f_w, \tag{2}$$

where,

$$M_1 = 1.13 - 0.09\left(\frac{a}{c}\right),$$

$$M_2 = -0.54 + \frac{0.89}{0.2 + (a/c)},$$

$$M_3 = 0.5 - \frac{1.0}{0.65 + (a/c)} + 14\left(1.0 - \frac{a}{c}\right)^{24},$$

$$g = 1 + \left[0.1 + 0.35\left(\frac{a}{t}\right)^2\right](1 - \sin\phi)^2,$$

$$f_\phi = \left[\left(\frac{a}{c}\right)^2 \cos^2\phi + \sin^2\phi\right]^{1/4},$$

and

$$f_w = \left[\sec\left(\frac{\pi c}{2b}\sqrt{\frac{a}{t}}\right)\right]^{1/2}.$$

The factor Q is given by the relation

$$Q = 1 + 1.464\left(\frac{a}{c}\right)^{1.65}, \quad \text{where } \left(\frac{a}{c}\right) \leqslant 1 \tag{3}$$

With the geometry coefficients determined, the stress intensity factor can be determined once the stress, crack depth and crack length are known. It should be noted that in Eq. (1), the stress quantity used is the amplitude between the maximum and minimum levels of loading; and so is the stress intensity factor.

3.2. Data

The data available for analysis from experiments and the SEM photographs covers the following variables:

- Crack depth (a): Initial crack depth is obtained from surface roughness condition resulting from applied sanding of samples within the critical area of failure before start of tests. Fig. 7 shows the surface roughness data after sanding. The value for initial crack depth (a_i) is 30 μm. Value for final crack depth (a_f) is measured for each sample from direct examination of samples and SEM photographs. So, it is different from sample to sample. Intermediate crack depth is measured for each sample directly from SEM photographs, by determining (Δa).
- Crack surface half length (c): It is measured directly from SEM micrographs by determining the ratio of depth to half length (a/c). This ratio is restricted to very deep cracks in order to avoid violation of the limit set by geometry factor validity requirements. The limit is set as $c \leqslant b$, where b is half the width of the specimen.
- Number of cycles (N): Final number of cycles (N_f) is obtained directly from test data, while intermediate values are determined from (ΔN), by measurement directly from SEM photographs. Due to the nature of material response to fatigue loading observed in tests, high number of cycles are observed before noticeable crack growth is detected. Also from SEM micrographs, it is noticed that, at the latter stage of loading, there is high crack growth compared to number of cycles. Based on this, it is assumed that one half of the total number of cycles is passed before noticeable crack growth is observed. This crack growth will be estimated by the thickness of the portion covered by the outer layer of the specimen, which, at the same time, blocks initial crack growth stage. Then, the number of cycles is calculated from a certain point and linked with the crack length associated with it.

3.3. Calculation procedure

The calculation procedure of the parameters needed to construct the Paris equation for the tested samples is summarized below.

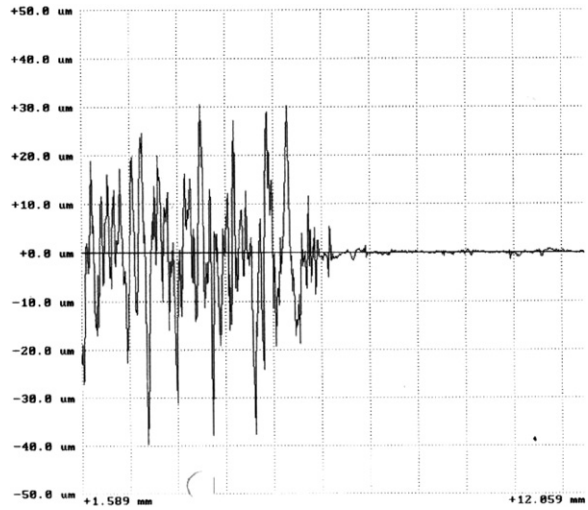

Fig. 7. The Surface profile for the sanded surface indicating a maximum roughness value up to 30 μm (on the left) compared to normal surface value not more than 3 μm as indicated on the right hand side of the graph.

(a) Obtain values of parameters and variables from the data tables available as follows:
- t: specimen thickness, mm.
- b: specimen half width, mm.
- a_s: initial crack depth, mm.
- a_f: final crack depth, mm.
- c_s: initial crack half length, mm.
- c_f: final crack half length, mm.
- N_f: final Number of cycles
- ΔP: load amplitude ($P_{max} - P_{min}$), kN.

(b) Obtain data for Δa and ΔN from SEM micrographs for a representative set of points. This is done by examination of the striations on the fracture surface of the test specimens, which correspond to fatigue cycles.

(c) Construct data points consisting of pairs of crack depth and number of cycles for history of loading (a_i, N_i) where i range is set from 1 to 5.

(d) Plot corresponding crack depth and number of cycles data to obtain the a–N curve.

(e) ASTM [9] recommended secant method for computing crack growth rate is adopted. In order to utilize this method, an average value of crack length, and corresponding number of cycles are used. The relation used is as follows:

$$\frac{da}{dN} = \frac{a_{i+1} - a_i}{N_{i+1} - N_i}. \tag{4}$$

(f) Evaluate $\frac{da}{dN}(N_i), \quad i = 1, 5.$

(g) Compute $\Delta K(a_i)$ for the specimen from ΔP, B, W and the geometry factor $Y(a, c)$.

(h) Estimation of stress intensity factor is obtained by approximating the crack to be semi-elliptical within an infinite plate the specimen, as was detailed in the previous section.

(i) Plot $(\Delta K(a_i), \frac{da}{dN}(N_i))$ on log–log scale.

(j) Fit straight line to the plot to get the Paris equation parameters: A and m as in the relation:

$$\frac{da}{dN} = A\Delta K^m. \tag{5}$$

From the procedure outlined above, the Paris equation for each test temperature can be constructed and, consequently, the fatigue fracture parameters can be obtained for each case.

4. Results and discussion

Using the estimation procedure illustrated previously, the results from the tests and analytic procedure are presented here. The graphs of the stress versus fatigue life (S–N curves) as well as Paris law curves will be analyzed for different cases of testing temperature.

4.1. S–N curves

Fig. 8a shows a semi-log graph of the stress versus fatigue life for all the specimens tested at three different temperatures: −20 °C, −10 °C, and the ambient room temperature 23 °C. Along with the data for each case, shown is a straight line fit that indicates the characteristics of each case. Fig. 8b shows the same result but on a log–log graph with the ramp test results included in the graph.

Form these graphs we can see that the S–N life for the material is affected by the reduction in temperature through the reduction in the stress level and increase in number of cycles to failure. These results are in accordance with the trend in higher temperature range. It is also noted that the sensitivity of load to number of cycles, which is represented by the slog of the semi-log curve is reduced at low temperatures.

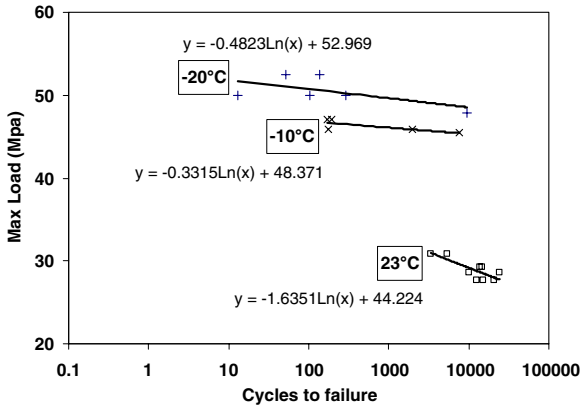

Fig. 8a. The semi-log *S–N* curve for all data at the three different temperatures (without inclusion of ramp test data).

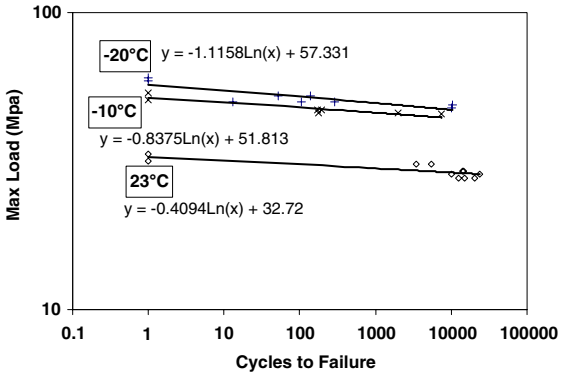

Fig. 8b. The log–log *S–N* curve for all data at the three different temperatures (with inclusion of ramp test data for each case).

4.2. Paris law parameters

From the calculation procedure discussed in the previous chapter, the stress intensity factor and the rate of change of crack length with respect to the number of cycles are obtained for the data points obtained for each sample. This is utilized to construct the Paris equation for each temperature case. Fig. 9a shows the result for samples 7 and 8, for the case of −20 °C. It is noted that data points for the two samples are in good agreement.

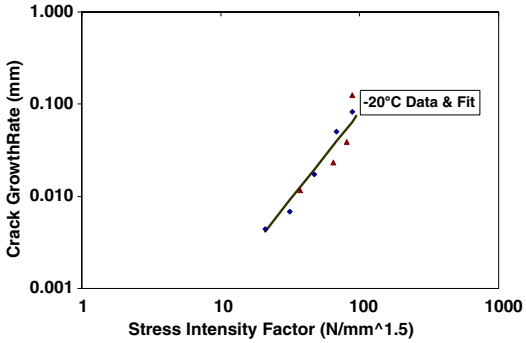

Fig. 9a. Paris law plot from test data for samples 7 and 8 for the case of −20 °C; and the straight line curve fitted to data.

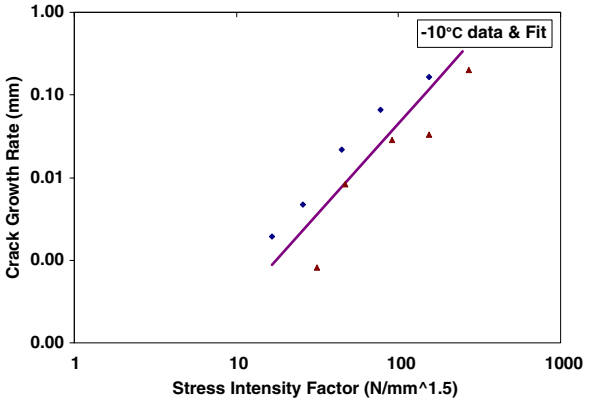

Fig. 9b. Paris law plot from test data for samples 20 and 22 for the case of −10 °C; and the straight line curve fitted to data.

The straight line fit for the two data sets is plotted; from which the Paris equation parameters can be obtained. From the graph the two constants are obtained as: $A = 0.000013$; and $m = 1.9$.

Fig. 9b shows the result for samples 20 and 22, for the case of −10 °C. In this case, it is noted that data points for the two samples are in good agreement it terms of the trend of the curve, although there is a slight shift between the two samples. The straight line fit for the two data sets is plotted as shown; and the Paris equation parameters are obtained as: $A = 0.000003$; and $m = 2.3$.

The results obtained here for the Paris law parameters are compared with results of the experimental work conducted by Grieg [3] on compact tension specimens of compression molded PVDF and those of Hertzberg et. al. [1] also for PVDF. The differences between the results of Grieg and Hertzberg work were attributed to the composition of the polymer as the one in the earlier work is a homo-polymer rather than the VF_2–CTFE copolymer used in the latter work. Fig. 10 shows the results obtained in the current work compared with the results mentioned above. Table 2 below shows the parameters for all cases presented in the figure.

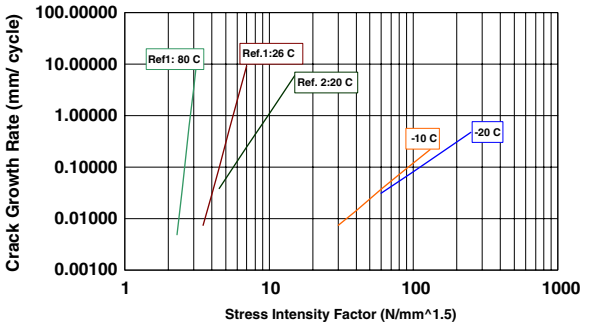

Fig. 10. Comparison of Paris law relations obtained in this work, from test data for temperatures of −10 °C and −20 °C, with those of Greig [3] (Ref. 1) and Hertzberg et al. [1] (Ref. 2).

Table 2
Fatigue fracture parameter of Paris equation for the cases compared in Fig. 10

Reference	Temperature (°C)	A	m
Grieg [3]	80	1.96×10^{-13}	24.604
Grieg [3]	26	5.829×10^{-10}	10.297
Hertzberg et. al. [1]	20	2.163×10^{-6}	4.209
−10 °C	−10	3.0×10^{-6}	2.3
−20 °C	−20	1.3×10^{-5}	1.9

It can bee seen that the trend of gradual reduction in the exponent parameter with decreasing temperature is captured in the current analysis, thus corroborating previous results, although relative differences are present because of the different test procedures. Moreover, the phenomenological observation of fractured samples which indicates change of the facture mode with decreasing temperature can be explained by this change in fatigue fracture parameters.

5. Conclusion

The aim of this work was to investigate the effect of temperature on the fatigue fracture behavior of polyvinylidiene fluoride especially at low temperatures, motivated by service application requirements. Using results of experimental work on short pipe sections of extruded PVDF, a procedure for estimating the crack parameters using a semi-elliptical surface crack assumption was performed; from which parameters of the Paris equation for fatigue fracture were obtained. The results capture the trend of the material behavior for high temperature.

Acknowledgement

A. Al-Abduljabbar acknowledges with gratitude the support of this work by the British Council in Riyadh through the Postgraduate Research Program Fund. We are grateful to Wellstream North Sea Ltd, for providing the PVDF fatigue data at 26 °C and 80 °C.

References

[1] Hertzberg RW, Manson JA, Skibo MD. Frequency sensitivity of fatigue processes in polymeric solids. Polym Eng Sci 1975;15(4):252–60.
[2] Hertzberg RW, Skibo MD, Manson JA. Fatigue crack propagation in polyacetal. J Mater Sci 1978;13:1038–44.
[3] Grieg JM. Fatigue testing of PVDF. Plastic Pipes Report, September 2001.
[4] Melve BJ. Principles for life time estimation of PVDF pressure barriers for high temperature flexible pipes based on fracture mechanics. In: Proceedings of 20th international conference on offshore mechanics and arctic engineering, Rio de Janeiro, Brazil, no. 2001-3575, 3–8th June, 2001.
[5] Gibson AG, Jerry P. A liner crack growth model for PVDF. RCID Report, University of Newcastle upon Tyne, 11 July 2002.
[6] Merah N, Saghir F, Khan Z, Bazoune A. A study of frequency and temperature effects on fatigue crack growth resistance of CPVC. Eng Fract Mech 2005;72:1691–701.
[7] Newman JC, Raju IS. An empirical stress-intensity factor equation for the surface crack. Eng Fract Mech 1981;15(1-2):185–92.
[8] Anderson TL. Fracture mechanics, fundamentals and applications. CRC Press; 1991.
[9] ASTM E 647-99. Standard test method for measurement of fatigue crack growth rates, September 1999.